



## Coumarin-based novel fluorescent zinc ion probe in aqueous solution



Jun Li<sup>†</sup>, Chun-Fang Zhang<sup>†</sup>, Ze-Zhong Ming, Ge-Fei Hao, Wen-Chao Yang<sup>\*</sup>,  
Guang-Fu Yang<sup>\*</sup>

Key Laboratory of Pesticide & Chemical Biology, College of Chemistry, Ministry of Education, Central China Normal University, Wuhan 430079, PR China

### ARTICLE INFO

#### Article history:

Received 23 December 2012  
Received in revised form 26 February 2013  
Accepted 8 March 2013  
Available online 14 March 2013

#### Keywords:

Coumarin  
Zn<sup>2+</sup>  
Fluorescent probe

### ABSTRACT

A novel coumarin-derived fluorescent probe, **FCP**, was designed for Zn<sup>2+</sup> quantification based on the photo-induced electron transfer (PET) mechanism. This probe selectively and sensitively detects Zn<sup>2+</sup> in aqueous solution with wide pH range. Large fluorescence enhancement (13-fold) was observed upon the addition of Zn<sup>2+</sup>. **FCP** also displays excellent cell permeability in HeLa cell model and very low cytotoxicity to HEK-293 cell model.

© 2013 Elsevier Ltd. All rights reserved.

## 1. Introduction

As the second most abundant transition metal essential for human health, zinc ion (Zn<sup>2+</sup>) has drawn considerable interest due to its broad biological functions, including modulation of catalytic activity of hundreds of specific enzymes, regulation of gene transcription, and involvement in brain pathology.<sup>1,2</sup> Abnormal concentrations of Zn<sup>2+</sup> are known to be closely related to several diseases, including chronic diarrhea, growth failure, immune deficiency, Alzheimer's disease.<sup>3,4</sup> In addition, with the development of modern industry, the environment pollution caused by transition metals like Zn<sup>2+</sup> has become more serious and pose a threat to human health and the environment.<sup>5</sup> Therefore, the accurate measurement of Zn<sup>2+</sup> concentrations in either the clinical setting or for environmental monitoring is of great importance.

Fluorescence emission spectrometry has emerged as one of the most popular methods for specific measurement because of its high sensitivity, simplicity, and real time monitoring without complicated pretreatment.<sup>6–9</sup> Numerous fluorescent probes for Zn<sup>2+</sup> detection have been developed by conjugating different kinds of fluorophores.<sup>10–18</sup> However, many of the existing Zn<sup>2+</sup> probes have poor water solubility, which prevents their applications in

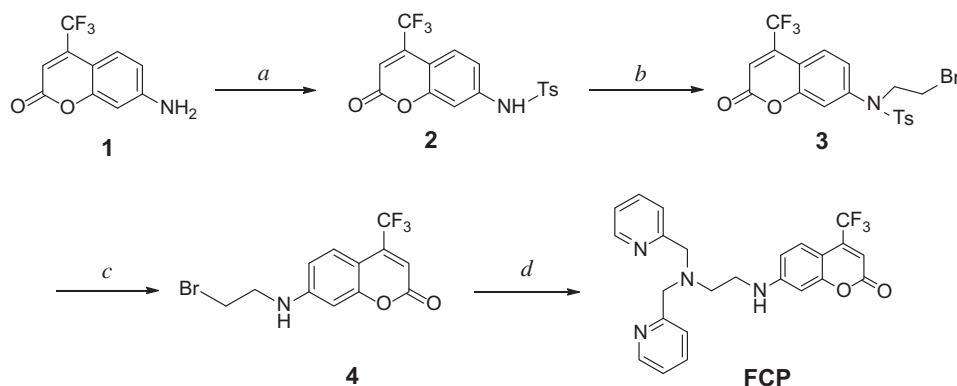
biological systems. Other probes can not be applied to living systems due to poor cell permeability. Thus, efforts directed toward the development of novel Zn<sup>2+</sup> probes are ongoing.

A fluorescent probe usually consists of two structural units: the receptor unit for specifically recognizing the target molecule or ion, and the fluorophore unit for translating the host–guest recognition into fluorescence signal.<sup>19,20</sup> Coumarins are widely used as effective fluorophores due to their high fluorescence quantum yield.<sup>13,21,22</sup> Furthermore, coumarin derivatives are usually easily synthesized and possess good water solubility, low cytotoxicity, and good cell permeability,<sup>23,24</sup> making them powerful chemical tools for studying biological systems. As one of the most commonly used chelators, di-2-picolylamine (DPA) is a classical membrane-permeable chelator with high selectivity for Zn<sup>2+</sup> over other alkali and alkaline-earth metal ions.<sup>25–27</sup> Usually, electronegative atoms, such as N,<sup>28</sup> O,<sup>29</sup> S,<sup>30</sup> were introduced to the fluorophore part of molecular probes as additional electron donors with the aim to improve the chelator's affinity toward metal ions. To the best of our knowledge, few coumarin-based DPA derivatives as fluorescent Zn<sup>2+</sup> chemical probes have been described until recently.<sup>31,32</sup>

Herein, based on the mechanism of photo-induced electron transfer (PET),<sup>20</sup> we designed and synthesized a coumarin-based DPA fluorescent probe (**FCP**) with high sensitivity and selectivity for zinc ion in aqueous solution (Scheme 1). We envisioned that fluorescence intensity would be greatly enhanced when **FCP**'s PET pathway was blocked upon the binding with Zn<sup>2+</sup>, which might be utilized to quantify Zn<sup>2+</sup> levels conveniently for healthcare and environmental monitoring.

<sup>\*</sup> Corresponding authors. Tel.: +86 27 6786 7706; fax: +86 27 6786 7141; e-mail addresses: [tomyang@mail.ccn.edu.cn](mailto:tomyang@mail.ccn.edu.cn) (W.-C. Yang), [gfyang@mail.ccn.edu.cn](mailto:gfyang@mail.ccn.edu.cn) (G.-F. Yang).

<sup>†</sup> These two authors made equal contributions.



Reagents and conditions: a, TsCl, pyridine, CH<sub>2</sub>Cl<sub>2</sub>, *r.t.*, 4 h; b, Br(CH<sub>2</sub>)<sub>2</sub>Br, Cs<sub>2</sub>CO<sub>3</sub>, CH<sub>3</sub>CN, reflux, 12 h; c, H<sub>2</sub>SO<sub>4</sub> (conc.), 90 °C; d, DPA, K<sub>2</sub>CO<sub>3</sub>, KI, CH<sub>3</sub>CN, reflux, 12 h

Scheme 1. Synthesis of the new fluorescent probe FCP.

## 2. Experimental

### 2.1. Reagents and instruments

Unless otherwise noted, all chemical reagents were commercially available and treated with standard methods before use. Silica gel column chromatography (CC): silica gel (200–300 mesh); Qingdao Makall Group Co., Ltd; Qingdao; China. Solvents were dried in a routine way and redistilled. <sup>1</sup>H NMR and <sup>13</sup>C NMR spectra were recorded in CDCl<sub>3</sub> or CD<sub>3</sub>CN-*d*<sub>3</sub> on a Varian Mercury 600 or 400 spectrometer and resonances (δ) are given in parts per million relative to tetramethylsilane (TMS). The following abbreviations were used to designate chemical shift multiplicities: s=singlet, d=doublet, t=triplet, m=multiplet, br=broad. High resolution mass spectra (HRMS) were acquired in positive mode on a WATERS MALDI SYNAPT G2 HDMS (MA, USA).

### 2.2. Synthesis and characterization of coumarin derivatives

**2.2.1. Synthesis of 7-[N-(*p*-toluenesulfonyl)amino]-4-trifluoromethylcoumarin.** 7-Amino-4-trifluoromethylcoumarin 3.71 g (16.2 mmol) was dissolved in dichloromethane (20 mL). After slow addition of the distilled pyridine (20 mL) and *p*-toluenesulfonyl chloride (6.80 g, 35.7 mmol), the mixture was then stirred for 4 h at room temperature. Then ethyl acetate 150 mL was added, followed by wash of citric acid solution for three times and brine once. The resulting solution was dried with sodium sulfate and evaporated, washed with a small portion of cooled dichloromethane and dried in vacuo to give the compound **2** as white solid.<sup>33</sup> Yield: 5.64 g (91%). Mp 193–194 °C. <sup>1</sup>H NMR (CDCl<sub>3</sub>, 400 MHz): δ 7.81 (d, *J*=8.0 Hz, 2H), 7.57 (d, *J*=8.8 Hz, 1H), 7.30 (d, *J*=8.0 Hz, 2H), 7.21 (d, *J*=2.4 Hz, 1H), 7.08 (dd, *J*<sub>1</sub>=2.0 Hz, *J*<sub>2</sub>=2.0 Hz, 1H), 6.67 (s, 1H), 2.40 (s, 3H). EI-MS: *m/z*, calcd 383.34, found 383.02.

**2.2.2. Synthesis of 7-[N-(2-bromoethyl)-N-(*p*-toluenesulfonyl)amino]-4-trifluoro-methyl coumarin.** A mixture of 7-Tosylamino-4-trifluoromethylcoumarin (3.2 g, 8.35 mmol), distilled acetonitrile (30 mL), cesium carbonate (4.06 g, 12.50 mmol), and 1, 2-dibromoethane (15.6 g, 83.5 mmol) was stirred for 12 h at 80 °C. After filtration, the solution was evaporated and purified by silica gel column chromatography to afford the compound **3** as white solid.<sup>33</sup> Yield: 2.28 g (81%). Mp 80–81 °C. <sup>1</sup>H NMR (CDCl<sub>3</sub>, 600 MHz): δ 7.71 (d, *J*=7.8 Hz, 1H), 7.51–7.50 (m, 2H), 7.31–7.24 (m, 3H), 7.10 (s, 1H), 6.82 (s, 1H), 3.94 (t, *J*=7.2 Hz, 2H), 3.43

(t, *J*=7.2 Hz, 2H), 2.45 (s, 3H). EI-MS: *m/z*, calcd 490.29, found 490.91.

**2.2.3. Synthesis of 7-[N-(2-bromoethyl)amino]-4-trifluoromethylcoumarin.** 7-(N-(2-Bromoethyl)-N-tosylamino)-4-trifluoromethylcoumarin (0.75 g, 1.53 mmol) was added to concentrated sulfuric acid 5 mL and the solution was stirred for 4 h at 90 °C. The reaction mixture was cooled and carefully poured into water. The blue solid was precipitated, followed by filtration and silica gel column chromatography to obtain the compound **4** as yellow solid.<sup>33</sup> Yield: 0.3 g (58%). Mp 151–152 °C. <sup>1</sup>H NMR (CDCl<sub>3</sub>, 400 MHz): δ 7.50 (d, *J*=7.2 Hz, 1H), 6.61 (d, *J*=8.8 Hz, 1H), 6.53 (s, 1H), 6.47 (s, 1H), 3.76 (t, *J*=5.6 Hz, 2H), 3.60 (t, *J*=5.6 Hz, 2H). EI-MS: *m/z*, calcd 336.10, found 336.96.

**2.2.4. Synthesis of probe FCP.** DPA (199 mg, 1 mmol), K<sub>2</sub>CO<sub>3</sub> (138 mg, 1 mmol), KI (166 mg, 1 mmol), intermediate **4** (168 mg, 0.5 mmol) were dissolved in distilled CH<sub>3</sub>CN, and the reaction mixture was stirred under reflux for 12 h. After removing the solvent under reduced pressure, the residue was then purified by silica column chromatography using CH<sub>2</sub>Cl<sub>2</sub>/CH<sub>3</sub>OH (100/1, *v/v*) to afford the final product as yellow oil. Yield: 91 mg (40%). IR (neat): 3392, 2921, 2851, 1643, 1466, 1260, 1094 cm<sup>-1</sup>; <sup>1</sup>H NMR (CDCl<sub>3</sub>, 400 MHz): δ 8.60 (d, *J*=4.4 Hz, 2H), 7.66–7.62 (m, 2H), 7.44 (d, *J*=8.8 Hz, 1H), 7.37 (d, *J*=8.0 Hz, 2H), 7.20–7.18 (m, 2H), 6.78 (s, 1H), 6.62 (dd, *J*<sub>1</sub>=2.4 Hz, *J*<sub>2</sub>=2.4 Hz, 1H), 6.41 (d, *J*=2.4 Hz, 1H), 6.37 (s, 1H), 3.96 (s, 4H), 3.22 (t, *J*=5.6 Hz, 2H), 2.96 (t, *J*=5.6 Hz, 2H). <sup>13</sup>C NMR (100 MHz, CDCl<sub>3</sub>): δ 160.55, 158.59, 157.10, 152.75, 149.03, 141.98, 141.64, 136.61, 125.82, 123.32, 122.28, 111.42, 107.41, 103.03, 97.47, 59.92, 51.84, 40.74. HRMS (ESI<sup>+</sup>) calcd for [FCP+H]<sup>+</sup>: calcd 455.1695, found: 455.1690.

### 2.3. Determination of quantum yield

The quantum yields of fluorescence were determined by comparison of the integrated area of the corrected emission spectrum of samples with a reference. Specifically, using fluorescein (Φ=0.98, 0.1 M H<sub>2</sub>SO<sub>4</sub>) as reference, FCP (10 μM) were prepared in 0.1 M phosphate (pH 7.0) buffer and diluted to certain solution to make their absorption less than 0.05. Then their UV–vis absorption spectrum was studied and the corresponding emission at relevant wavelength of excitation was measured as well. After correction of the refractive index of the different solvents determined by Abbe's refractometer, the quantum yields were calculated with the expression in following equation.

$$\phi_s = \frac{F_s \cdot A_c}{F_c \cdot A_s} \phi_c$$

#### 2.4. Determination of association constant

Based on Job's method, fluorescence spectroscopy was used to determine the apparent association constant ( $K_a$ ) of **FCP** with  $Zn^{2+}$ . As shown in Fig. 1b, two series of solutions containing certain  $Zn^{2+}$  and **FCP** were prepared, in which their total concentrations are constants. Fluorescence intensity of those mixtures of  $Zn^{2+}$  and **FCP** in varying molar ratios (1:9, 2:8, 3:7, 4:6, 5:5, 6:4, 7:3, 8:2, 9:1) were measured. Then the  $K_s$  can be calculated by fitting the data to the following equation, where  $a_1, b_1, a_2, b_2$  are the initial concentration of metal ions and ligand concentration,  $X$  is the equilibrium concentration of complex.

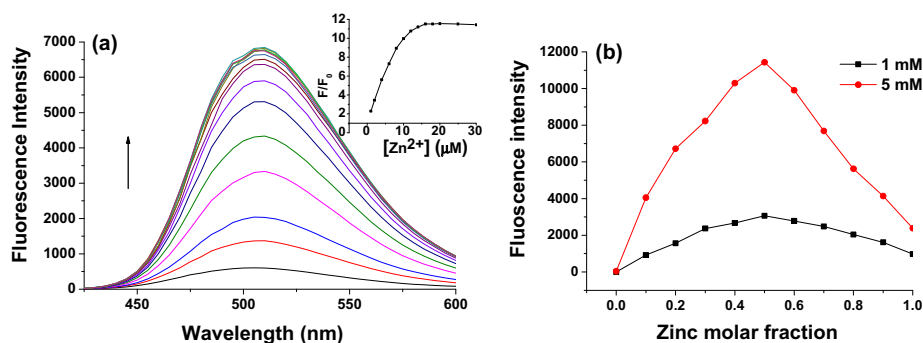


**Fig. 1.** (a) Fluorescence spectra of **FCP** ( $\lambda_{ex}=390$  nm,  $\lambda_{em}=510$  nm) in the presence of different concentrations of  $Zn^{2+}$ , and both the excitation and emission slit widths were 5 nm. (b) The Job plots for binding between **FCP** and  $Zn^{2+}$  evaluated from the fluorescence with a total concentration of 1 mM and 5 mM, respectively. Inset in panel (a): Fluorescence titration profile versus concentration of  $Zn^{2+}$  in 0.1 M phosphate buffer (pH 7.0).

$$K_a = \frac{X}{(a_1 - X)(b_1 - X)} = \frac{X}{(a_2 - X)(b_2 - X)}$$

#### 2.5. Imaging of HeLa cells

HeLa cells were cultured in DMEM media supplemented with 10% (v/v) fetal bovine Serum, 1% (v/v) 100 mM Sodium Pyruvate (Gibco). The cells were seeded at  $0.3 \times 10^6$  cells/ml in the culture media, incubated at 37 °C, 5%  $CO_2$ . Then 20  $\mu M$   $ZnCl_2$  was added into the cells and the cells were incubated for 12 h at 37 °C. Later, the samples were washed twice to remove the remaining zinc ions, followed by the treatment of 10  $\mu M$  **FCP** in the culture media containing 0.1% (v/v) DMSO. After 1 h incubation, the treated cells were imaged by confocal laser scanning microscopy (CLSM).

#### 2.6. Quantum chemical calculation

Initial structures of **FCP**, **FCP**<sup>-</sup>,  $[Zn(\mathbf{FCP})]^{2+}$ ,  $[Zn(\mathbf{FCP})]^+$  were constructed in SYBYL-X 1.1 software and optimized using Tripos force field. The density functional theory (DFT) calculations were carried out by using Gaussian 03 program. Ground state geometry optimization were performed with the basis set of B3LYP 6-31+G (d, p). The resulting geometries were used energy calculation of HOMOs and LUMOs.

### 3. Results and discussion

#### 3.1. Fluorescence detection in aqueous solution and related mechanism

Starting with 7-amino-4-trifluoromethylcoumarin and DPA,<sup>12,33,34</sup> the new sensor **FCP** was synthesized in a straightforward manner;

the synthetic details are shown in Scheme 1 and the relevant spectra are depicted in Supplementary data.

The spectroscopic properties and the metal-binding behavior of the newly synthesized probe were measured in 0.1 M phosphate buffer (pH 7.0) at 30 °C. The peak of UV–vis absorption spectrum for **FCP** was located at 390 nm (Fig. S1). Using 390 nm as the excitation wavelength, **FCP** itself exhibited weak intensity of fluorescence emission at 510 nm ( $\Phi=0.15$ , Fig. 1a). Upon addition of free  $Zn^{2+}$  ion, the fluorescence intensity ( $F/F_0$ ) of **FCP** increased promptly, and the maximum fluorescence intensity ( $F/F_0$ ) enhancement increased by 13-fold when 1 equiv of  $Zn^{2+}$  ( $\Phi=0.47$ ) was added. This resultant high quantum yield is quite comparable with the existing  $Zn^{2+}$  fluorescent probes in aqueous solution.<sup>22,23</sup>

The titration curve in Fig 1a indicated that the binding stoichiometry between **FCP** and  $Zn^{2+}$  is 1:1. To further understand the

mode of complexation, <sup>1</sup>H NMR spectra studies were undertaken using  $CH_3CN-d_6$  as the solvent in the absence and presence of  $Zn^{2+}$  (Fig. 2). The protons at the *ortho* position of the pyridines were downfield shifted from 8.44 to 8.55 ppm by the *N*-metal coordination effect upon the addition of  $Zn^{2+}$ . Similar shifts were observed for the protons at the 2-, 3-, and 4-positions of pyridines, and the H atoms at the 5-position in the DPA moiety were split and downfield shifted. In addition, density functional theory (DFT) calculations were performed to gain further structural insight into the mechanism. As depicted in Fig. 3, the HOMO–LUMO energy gap decreased about 0.28 eV once **FCP** bound with  $Zn^{2+}$  whereas the HOMO–LUMO energy gap increased slightly by approximately 0.03 eV for the coordination between **FCP**- and  $Zn^{2+}$ . DFT analysis revealed that  $[Zn(\mathbf{FCP})^{2+}]$  preferentially occurred while  $[Zn(\mathbf{FCP})^+]$  was not favorable, which is consistent with the experimental observations of PET phenomena other than internal charge transfer (ICT). Furthermore, the detection limit ( $S/N=3$ ) was about 0.44  $\mu M$  as based on the calculation of the titration curve. According to the method described above, the apparent association constant ( $K_a$ ) of **FCP** for  $Zn^{2+}$  was determined to be about  $4.10 \times 10^5 M^{-1}$ .

After confirming the sensitivity of **FCP**, we also investigated the interference of other bio-relevant metal ions, and the results were summarized in Fig. 4a.  $Ca^{2+}$ ,  $Mg^{2+}$ ,  $K^+$ , and  $Na^+$ , which are much more abundant in the biosphere, did not trigger any fluorescence enhancement even at very high concentrations (1 mM, 100 times higher than the concentration of **FCP**). In addition, no significant change of fluorescence emission intensity was observed upon the addition of some first row heavy and transition metal (HTM) ions, such as  $Mn^{2+}$ ,  $Pb^{2+}$ ,  $Ci^{3+}$ , and  $Fe^{3+}$ . Other first row transition metal ions like  $Cu^{2+}$ ,  $Co^{2+}$ , and  $Ni^{2+}$  quenched the fluorescence, probably due to their empty d-orbitals when they bind with **FCP**.<sup>35</sup> In contrast,  $Cd^{2+}$  and  $Hg^{2+}$  displayed obvious interference to the detection of  $Zn^{2+}$  because they are in the same group of metals as

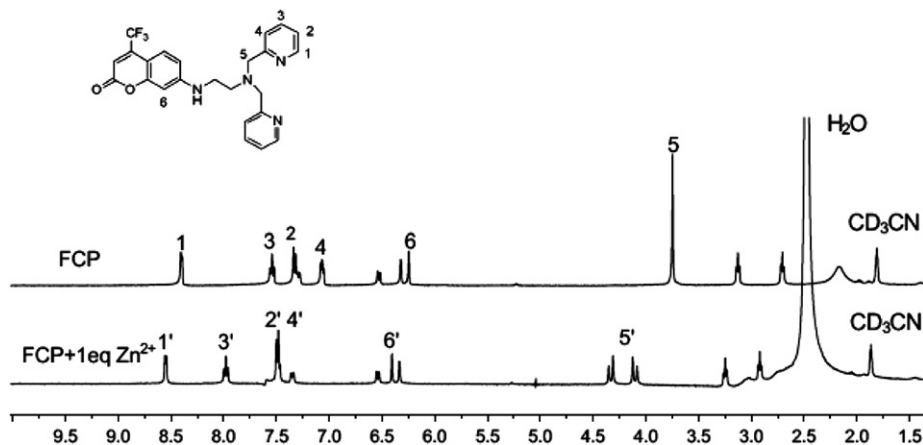


Fig. 2.  $^1\text{H}$  NMR spectra of **FCP** (1 mM) in the absence and presence of  $\text{Zn}^{2+}$  (1 equiv) in  $\text{CD}_3\text{CN}-d_3$ .

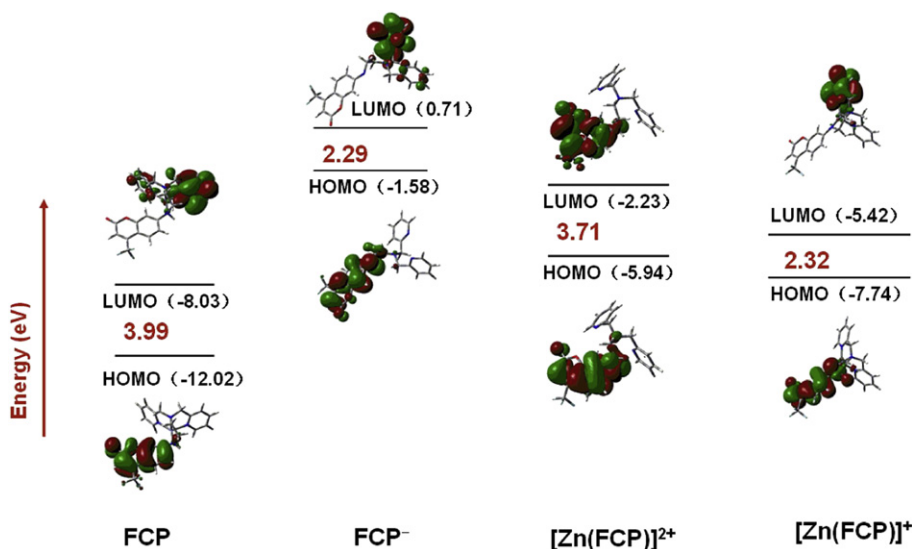


Fig. 3. The HOMOs and LUMOs of **FCP**, **FCP** $^-$ , **[Zn(FCP)] $^{2+}$**  and **[Zn(FCP)] $^+$** .

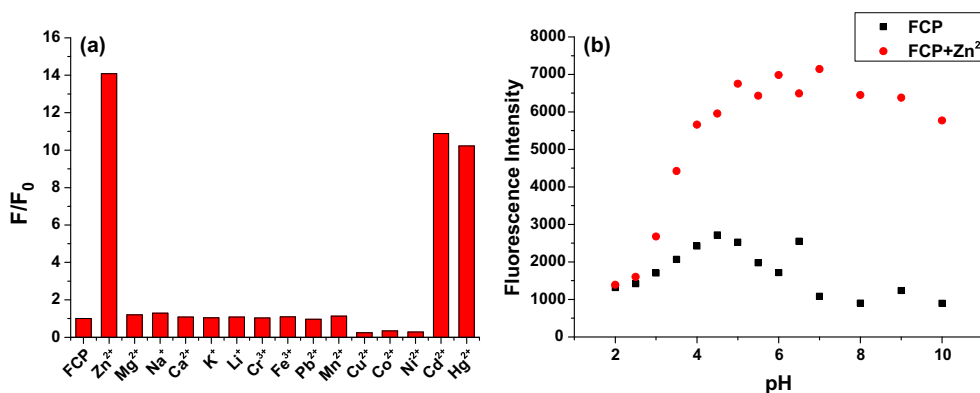


Fig. 4. (a) Fluorescence responses of 10  $\mu\text{M}$  **FCP** to various metal ions in 0.1 M phosphate buffer (pH 7.0) at the excitation wavelength of 390 nm. Among those bio-relevant metals ions,  $\text{Ca}^{2+}$ ,  $\text{Mg}^{2+}$ ,  $\text{K}^+$ ,  $\text{Na}^+$ , and  $\text{Li}^+$  were added at 100 equiv and the rest were introduced at 10 equiv. (b) The pH dependence of **FCP** (10  $\mu\text{M}$ ) in the absence and presence of  $\text{Zn}^{2+}$  (100  $\mu\text{M}$ ).

$\text{Zn}^{2+}$  in the periodic table, but the fluorescence intensity upon their addition was lower than that of  $\text{Zn}^{2+}$  at the same dosage. Considering their low concentrations in typical biological systems, **FCP** should still be suitable for the accurate quantification of the concentration of  $\text{Zn}^{2+}$  in biological system.

The influence of pH on the fluorescence response of **FCP** was also examined in different phosphate buffers (Fig. 4b). The resulting fluorescence change of **FCP** alone was not especially dependent on pH, which means both the chemical structure and fluorescence property of **FCP** are relatively stable over a broad range from pH 2.0

to pH 10.0. As for the fluorescence emission of **FCP** in the presence of 10 equiv  $\text{Zn}^{2+}$ , the fluorescence was enhanced as the pH increased and reached the maximum intensity at pH 6.0. The kinetic change of the pH dependence of **FCP**– $\text{Zn}^{2+}$  complex can be attributed to: (1) the amine group in DPA will be protonated in low pH solutions, which would hinder the binding between **FCP** and  $\text{Zn}^{2+}$ ; and (2) in neutral solution or a high pH environment, the free amine group in DPA can easily form strong interactions with  $\text{Zn}^{2+}$ . The above study demonstrated that **FCP** could be applied to track the  $\text{Zn}^{2+}$  levels in aqueous solutions with pH values ranging from 6.0 to 9.0.

### 3.2. Living cell imaging

To further study the cell permeability and the in vivo coordination capability, a preliminary study of **FCP** in living human HeLa cells was performed using confocal laser scanning microscopy (CLSM). As shown in Fig. 5, compared to the controls with either **FCP** (10  $\mu\text{M}$ ) or  $\text{Zn}^{2+}$  (20  $\mu\text{M}$ ), much stronger green fluorescence was observed in cells with the sequential addition of both **FCP** (10  $\mu\text{M}$ ) and  $\text{Zn}^{2+}$  (20  $\mu\text{M}$ ). These results indicate that **FCP** has excellent cell permeability and could efficiently bind with  $\text{Zn}^{2+}$  in vivo.

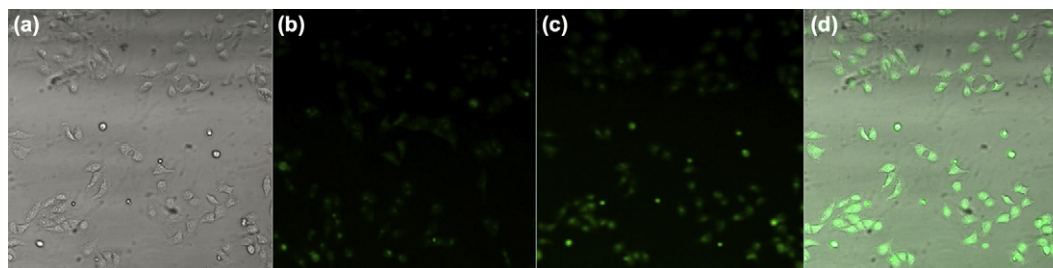


**Fig. 5.** (a) Brightfield image of HeLa cells. (b) CLSM image of HeLa cells only labeled with **FCP** (10  $\mu\text{M}$ ) after incubation for 30 min. (c). CLSM image of HeLa cells after sequential treatment with 20  $\mu\text{M}$   $\text{Zn}^{2+}$  and 10  $\mu\text{M}$  **FCP**. (d). Merged image of (a) and (c).

In addition, the cytotoxicity of **FCP** had been investigated in normal human embryonic kidney (HEK-293) cells by the MTT assay. HEK-293 cells were seeded at  $1 \times 10^5$  cells per well in 24-well plates and incubated for 24 h before treatment, followed by exposure to different concentrations (0  $\mu\text{M}$ , 0.1  $\mu\text{M}$ , 1  $\mu\text{M}$ , 5  $\mu\text{M}$ , 10  $\mu\text{M}$ , 20  $\mu\text{M}$ , 50  $\mu\text{M}$ , 100  $\mu\text{M}$ ) of **FCP** for additional 24 h. Cell samples then were incubated with MTT solution for 4 h, and after removal of the MTT

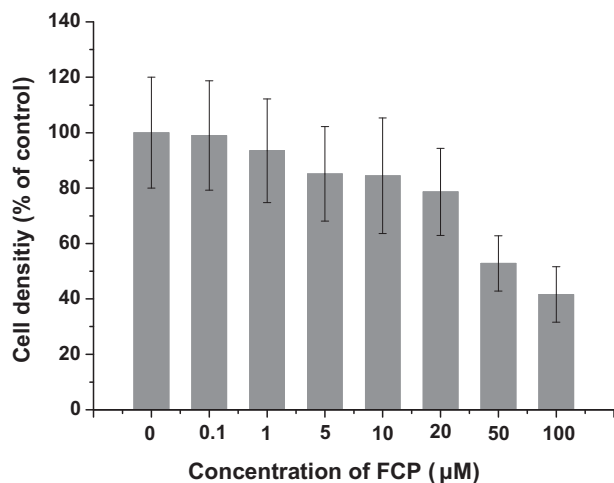


**Fig. 6.** Cytotoxic effects of different concentrations of **FCP** in HEK-293 cells after 24 h incubation.

solution, dimethyl sulfoxide was added to dissolve the formazan crystals. The absorbance was measured at  $\text{OD}_{540}$  with microplate reader. Each experiment was performed at least three times. As depicted in Fig. 6, the cytotoxic effect of **FCP** was assessed through the ratio of absorbances of **FCP** treated versus the control. It revealed that the cells remained in good condition when treated with **FCP** at a dosage of 20  $\mu\text{M}$  for as long as 24 h.

### 4. Conclusion

In summary, we have successfully designed and synthesized a novel ‘turn-on’ fluorescent probe **FCP** with excellent water solubility by combining coumarin as fluorophore and DPA as chief recognition unit. **FCP** displayed strong affinity to  $\text{Zn}^{2+}$  and produced great fluorescence enhancement due to the blocking of the PET process upon the binding of  $\text{Zn}^{2+}$ . In addition, **FCP** possesses much better quantum yield compared to most existing  $\text{Zn}^{2+}$  sensors that have been used in 100% aqueous solution. Although interference by other ions was observed, such as fluorescence quenching by three bivalent metal cations ( $\text{Co}^{2+}$ ,  $\text{Ni}^{2+}$ , and  $\text{Cu}^{2+}$ ) and significant fluorescence enhancement by two bivalent metal cations ( $\text{Hg}^{2+}$  and  $\text{Cd}^{2+}$ ), these interferences could be ignored due

to the very low concentrations of these ions in vivo. Furthermore, both the distinguished cell permeability and low toxicity demonstrated that **FCP** has great potential for reliable quantification of  $\text{Zn}^{2+}$  in biological systems.

### Acknowledgements

The research was supported in part by the National Basic Research Program of China (No. 2010CB126103) and the NSFC (No. 20925206, 21172091, and 21102052).

### Supplementary data

Supplementary data related to this article can be found at <http://dx.doi.org/10.1016/j.tet.2013.03.032>. These data include MOL files and InChIKeys of the most important compounds described in this article.

### References and notes

- Frederickson, C. J.; Koh, J. Y.; Bush, A. I. *Nat. Rev. Neurosci.* **2005**, *6*, 449–462.
- Bush, A. I.; Pettingell, W. H.; Multhaup, G.; d Paradis, M.; Vonsattel, J. P.; Gusella, J. F.; Beyreuther, K.; Masters, C. L.; Tanzi, R. E. *Science* **1994**, *265*, 1464–1467.
- Frederickson, C. J.; Bush, A. I. *BioMetals* **2001**, *14*, 353–366.
- Frederickson, C. J.; Hernandez, M. D.; McGinty, J. F. *Brain Res.* **1989**, *480*, 317–321.
- Yang, Z.; Yan, C.; Chen, Y.; Zhu, C.; Zhang, C.; Dong, X.; Yang, W.; Guo, Z.; Lu, Y.; He, W. *Dalton Trans.* **2011**, *40*, 2173–2176.
- Moragues, M. E.; Martinez-Manez, R.; Sancenon, F. *Chem. Soc. Rev.* **2011**, *40*, 2593–2643.
- Xu, Z.; Yoon, J.; Spring, D. R. *Chem. Soc. Rev.* **2010**, *39*, 1996–2006.

8. Duke, R. M.; Veale, E. B.; Pfeffer, F. M.; Kruger, P. E.; Gunnlaugsson, T. *Chem. Soc. Rev.* **2010**, *39*, 3936–3953.
9. Jiang, W.; Fu, Q.; Fan, H.; Wang, W. *Chem. Commun.* **2008**, 259–261.
10. Kwon, J. E.; Lee, S.; You, Y.; Baek, K. H.; Ohkubo, K.; Cho, J.; Fukuzumi, S.; Shin, I.; Park, S. Y.; Nam, W. *Inorg. Chem.* **2012**, , <http://dx.doi.org/10.1021/ic300476e>
11. Li, Y.; Shi, L.; Qin, L. X.; Qu, L. L.; Jing, C.; Lan, M.; James, T. D.; Long, Y. T. *Chem. Commun.* **2011**, 4361–4363.
12. Gordo, J.; Avo, J.; Parola, A. J.; Lima, J. C.; Pereira, A.; Branco, P. S. *Org. Lett.* **2011**, *13*, 5112–5115.
13. Ray, D.; Bharadwaj, P. K. *Inorg. Chem.* **2008**, *47*, 2252–2254.
14. Huang, S.; Clark, R. J.; Zhu, L. *Org. Lett.* **2007**, *9*, 4999–5002.
15. Yang, D.; Wang, H. L.; Sun, Z. N.; Chung, N. W.; Shen, J. G. *J. Am. Chem. Soc.* **2006**, *128*, 6004–6005.
16. Wang, P.; Liu, J.; Lv, X.; Liu, Y.; Zhao, Y.; Guo, W. *Org. Lett.* **2012**, *14*, 520–523.
17. Kiyose, K.; Kojima, H.; Urano, Y.; Nagano, T. *J. Am. Chem. Soc.* **2006**, *128*, 6548–6549.
18. Wu, Y.; Peng, X.; Guo, B.; Fan, J.; Zhang, Z.; Wang, J.; Cui, A.; Gao, Y. *Org. Biomol. Chem.* **2005**, *3*, 1387–1392.
19. Martinez-Manez, R.; Sancenon, F. *Chem. Rev.* **2003**, *103*, 4419–4476.
20. De Silva, A. P.; Gunaratne, H. Q.; Gunnlaugsson, T.; Huxley, A. J.; McCoy, C. P.; Rademacher, J. T.; Rice, T. E. *Chem. Rev.* **1997**, *97*, 1515–1566.
21. Lin, S. L.; Kuo, P. Y.; Yang, D. Y. *Molecules* **2007**, *12*, 1316–1324.
22. Kulatililke, C. P.; de Silva, S. A.; Eliav, Y. *Polyhedron* **2006**, *25*, 2593–2596.
23. Xu, Z.; Liu, X.; Pan, J.; Spring, D. R. *Chem. Commun.* **2012**, 4764–4766.
24. Kim, H. J.; Park, J. E.; Choi, M. G.; Ahn, S.; Chang, S. K. *Dyes Pigm.* **2010**, *84*, 54–58.
25. Ding, Y.; Xie, Y.; Li, X.; Hill, J. P.; Zhang, W.; Zhu, W. *Chem. Commun.* **2011**, 5431–5433.
26. Chen, M.; Lv, X.; Liu, Y.; Zhao, Y.; Liu, J.; Wang, P.; Guo, W. *Org. Biomol. Chem.* **2011**, *9*, 2345–2349.
27. Xue, L.; Wang, H. H.; Wang, X. J.; Jiang, H. *Inorg. Chem.* **2008**, *47*, 4310–4318.
28. Chen, X. Y.; Shi, J.; Li, Y. M.; Wang, F. L.; Wu, X.; Guo, Q. X.; Liu, L. *Org. Lett.* **2009**, *11*, 4426–4429.
29. Xu, Z.; Han, S. J.; Lee, C.; Yoon, J.; Spring, D. R. *Chem. Commun.* **2010**, 1679–1681.
30. Nolan, E. M.; Ryu, J. W.; Jaworski, J.; Feazell, R. P.; Sheng, M.; Lippard, S. J. *J. Am. Chem. Soc.* **2006**, *128*, 15517–15528.
31. Buccella, D.; Horowitz, J. A.; Lippard, S. J. *J. Am. Chem. Soc.* **2011**, *133*, 4101–4114.
32. Mizukami, S.; Okada, S.; Kimura, S.; Kikuchi, K. *Inorg. Chem.* **2009**, *48*, 7630–7638.
33. Mizukami, S.; Nagano, T.; Urano, Y.; Odani, A.; Kikuchi, K. *J. Am. Chem. Soc.* **2002**, *124*, 3920–3925.
34. Minami, T.; Matsumoto, Y.; Nakamura, S.; Koyanagi, S.; Yamaguchi, M. *J. Org. Chem.* **1992**, *57*, 167–173.
35. Moriuchi-Kawakami, T.; Hisada, Y.; Shibutani, Y. *Chem. Cent. J.* **2010**, *4*, 1–7.